Right heart chambers longitudinal strain provides enhanced diagnosis and categorization in patients living with pulmonary hypertension

Nilda Espinola-Zavaleta[1], Neftali Antonio-Villa[2], Enrique Guerra[3], Navin C. Nanda[4], Lawrence Rudski[4], Ricardo Alvarez-Santana[5], Gyselle Camacho-Camacho[6], Alberto Aranda-Fraustro[6], Jorge Cossio-Aranda[4], Karina Zamora[4], Diego Oregel-Camacho[6], Javier Armenta-Moreno[7], Joaquin Berarducci[7], and Erick Alexanderson-Rosas[6]

[1]Instituto Nacional de Cardiología
[2]UNAM Facultad de Medicina
[3] Universidad Nacional Autonoma de Mexico
[4]Affiliation not available
[5]Autonomous University of Ciudad Juarez
[6]National Institute of Cardiology Ignacio Chavez
[7]Instituto Nacional de Cardiologia Ignacio Chavez

April 05, 2024

Abstract

BACKGROUND: Increased systolic pulmonary artery pressure (sPAP) could lead to mechanical dysfunction and myocardial fibrosis of right heart chambers. Echocardiographic strain analysis has not been adequately studied in patients living with pulmonary hypertension (PH). METHODS AND RESULTS: A cross-sectional cohort of patients with suspected PH and echocardiographic strain evaluation was recruited. Cut-off values of peak tricuspid regurgitation velocity with low probability of PH ([?] 2.8 m/s), intermediate probability (2.9-3.4 m/s, without other echo PH signs) and high probability of PH (2.9-3.4 m/s with other echo PH signs and >3.4 m/s) categories were studied by right ventricular and right atrial strain analysis in a sample of 236 patients, 58 (56.9%) had low, 15 (14.7%) intermediate, and 29 (28.4%) high probability of PH. We observed a negative association between right ventricular free wall strain and atrial global strain with sPAP. As PH severity increased, right atrial reservoir, conduit, and contraction (booster) strain values decreased. Identified cut-off values of strain parameters had an adequate ability to detect PH severity categories In addition, post-mortem biopsies of right heart chambers from subjects with known severe pulmonary hypertension were analyzed to quantify myocardial fibrosis. Our sample of right heart biopsies (n=12) demonstrated an association between increased sPAP before death and right ventricular and right atrial fibrosis. CONCLUSIONS: Mechanical dysfunction and fibrosis in right chambers is associated with increased sPAP. Right ventricular and atrial strain could provide enhancement in the diagnosis and categorization of subjects with suspected PH.

INTRODUCTION

Echocardiography remains a fundamental clinical imaging tool for the assessment of the right heart ventricle (RV). Conventional echocardiographic parameters used in daily clinical practice that evaluate RV systolic function include tricuspid annular plane systolic excursion (TAPSE), the maximum velocity of the tricuspid lateral annulus during systole or the S wave (S') and RV fractional area change (RVFAC) (1). All these echocardiographic parameters have well known limitations (2). Assessment of right ventricular free wall longitudinal strain (RV-FWS) by two-dimensional echocardiographic speckle tracking analysis has overcome

some of these limitations and has emerged as a feasible and reproducible parameter to evaluate RV systolic function (3,4). RV-FWS has demonstrated good prognostic value in different clinical scenarios such as heart failure, and congenital heart disease (3). Nonetheless, RV-FWS and RA global longitudinal strain (RA-GS) have not been fully explored in a broad variety of pathologies (5,6,7,8. In patients with pulmonary hypertension, RV-FWS has been shown to be a potential predictor of major cardiovascular events. Moreover, its validation has been assessed with gold-standard methods such as cardiac magnetic resonance imaging (CMR) (9). However, to date, the diagnostic and predictive value of RV-FWS and RA-GS in pulmonary hypertension has not been fully explored. The use of right heart strain parameters in a clinical setting could broaden the stratification and overall, bring relevant information for care providers in patients with pulmonary hypertension. Furthermore, the evaluation of the long-standing effect of increased systolic pulmonary arterial pressure (sPAP) and myocardial fibrosis of the right heart chambers could support the hypothesis that myocardial deformation should be promptly tested in early stages of patients with pulmonary hypertension. Therefore, this study aims to assess the relationship and diagnostic performance of RV and RA strain to detect and evaluate sPAP parameters and stratify pulmonary hypertension categories. Furthermore, we extracted post-mortem sample biopsies to measure the degree of myocardial fibrosis in 12 patients classified with severe pulmonary hypertension to establish the association of increased sPAP with fibrosis.

METHODS

Study population cohorts

We designed a cross-sectional study in which we recruited consecutive patients who were evaluated in the Nuclear Cardiology Department (NCD) at the National Institute of Cardiology Ignacio Chavez, between the period of June 2018 to December 2019. The patients attended our institution's outpatient clinic due to dyspnea on exertion, fatigue, and dizziness and were sent for a transthoracic echocardiogram for further evaluation. All patients underwent conventional two-dimensional and Doppler transthoracic echocardiography, along with velocity vector imaging to assess the right heart chamber strain parameters. We excluded subjects with congenital heart diseases, prior myocardial infarction, sarcoidosis, mild or severe valvular disease, or subjects classified with unspecified cardiomyopathies. Patients with low echocardiographic image quality were excluded in the final analysis. We defined a control group which comprised of subjects who had normal pulmonary artery pressure values by echocardiographic measurement of peak tricuspid regurgitation velocity within our cohort sample. To assess inter-rater reliability and reproducibility of echocardiographic sPAP parameters, thirteen selected subjects from our first cohort were assessed at heart catheterization performed 10 days after the echocardiographic study. Written informed consent was obtained from all participants.

Echocardiographic assessment

We performed a complete conventional transthoracic echocardiogram with subjects in left lateral decubitus using a Siemens Acuson SC 2000 (Mountain View, California-USA) echocardiographic equipment with a phased array transducer. The right ventricular end-diastolic diameter was measured in the apical four-chamber view, below the tricuspid valve. The RV wall thickness was measured by 2D echocardiography in the subcostal four-chamber view. Right atrial (RA) volume was obtained using a single-plane method of disks in the apical four-chamber view at ventricular end-systole, and it was indexed by body surface area. The measurements of right ventricular fractional area change (RVFAC), tricuspid annular plane systolic excursion (TAPSE), tricuspid S-wave velocity, Tei index, E, A-wave velocities (rapid filling and atrial contribution, respectively), E/A ratio, and tricuspid E/e' ratio were obtained according to the guidelines of the American Society of Echocardiography and the European Association of Echocardiography (5,10,11).

Pulmonary arterial pressure assessment

The sPAP was calculated by peak tricuspid regurgitation velocity (TRV) with continuous-wave Doppler in the apical four-chamber view, using the simplified Bernoulli equation: $4 \times (\text{maximal TRV})^{2}$ + right atrial pressure. Right atrial pressure was estimated in the subcostal view according to inferior vena cava (IVC) size and collapsibility following a normal sniff: An IVC diameter < 2.1 cm that collapsed $>50\%$ with a sniff suggested normal RA pressure of 3 mm Hg (range, 0–5 mm Hg), whereas an IVC diameter > 2.1 cm that

collapsed < 50% with a sniff suggested a high RA pressure of 15 mm Hg (range, 10–20 mm Hg). In scenarios in which IVC diameter and collapse did not fit this paradigm, an intermediate value of 8 mm Hg (range, 5–10 mm Hg) might be used, or, preferably, other indices of RA pressure could be integrated to downgrade or upgrade to the standard or high values of RA pressure (5,11). The echocardiographic probability of pulmonary hypertension was classified as (1) low: peak TR velocity [?] 2.8 m/s, (2) intermediate: peak TRV 2.9-3.4 m/s, without other echo PH signs and (3) high: peak TRV 2.9-3.4 m/s with other echo PH signs and >3.4 m/s, based on the 2015 ESC/ERS Guidelines for the diagnosis and treatment of pulmonary hypertension (12).

Echocardiographic Strain Assessment

Strain assessment was performed off-line using vector velocity imaging (Siemens Acuson SC 2000, version 5). All images analyzed were obtained at 50-80 frames per second at end expiration. The region of interest was traced with a point-and-click approach on the endocardium of the RV free wall at end-diastole in the RV-focused apical four-chamber view. A broader region of interest was subsequently generated and manually adjusted if necessary. The Program automatically divided the RV free wall into three segments and performed the analysis of the deformation frame by frame. This process allowed an automated confirmation of the contour and generated deformation values. The peak strain values from the three free wall segments were averaged, and the mean value was taken as the RV free wall strain (RVFWS) (5,7,11, 12, 13).

For the right atrium (RA), the endocardial border was traced in the apical 4-chamber view, excluding the appendage and the Eustachian valve from the RA cavity. RA longitudinal strain curves were generated throughout the cardiac cycle with R-R gating. Accuracy of the automated border tracking was verified and manually adjusted if needed. Tracking was repeated three times, and averages were used for analysis as reported in guidelines (5,8, 11). The peak RA reservoir strain in ventricular systole, conduit strain in early diastole and peak contractile phase strain during atrial systole/ late diastole were measured and expressed as percentage. RA total reservoir phase and RA contractile phase were assessed by measuring the corresponding peak strains. The conduit strain was calculated as the difference between RA total reservoir strain and RA contractile strain (**Figure 1**).

To assess intra- and inter-observer reproducibility of RA reservoir, conduit, and contractile strain, thirteen randomly sampled analyses were repeated twice by the same observer and by a second observer without knowledge of previous findings, respectively.

Post-mortem right heart sample cohort

A second cohort of twelve biopsies of the right heart chambers from postmortem heart samples of patients diagnosed when living as severe pulmonary hypertension were included. This cohort was created to evaluate the hazard effect of increased systolic pulmonary artery pressure (sPAP) on the development of fibrosis in the right heart chambers.

The heart was photographed, and the macroscopic characteristics were taken, and sections were made for histological study. Samples were taken from the right atrial and the right ventricular free walls. We took photographs of the longitudinal section from the atrium's anterior wall, from the origin of the appendage to the tricuspid valve, and a transverse section of the ventricle in the middle portion of the free wall, covering the entire thickness of the wall.

The samples were processed with the histological technique of "paraffin inclusion". They were stained with the Masson technique to quantify the percentage of right atrial and right ventricular fibrous tissue, dividing the field of observation of the microscope into quarters. Two independent observers gave the percentage values, and a consensus value was obtained when there were differences. Microscopic photographs were taken of the most representative areas (**Figures 2-3**).

The study was carried out following the Declaration of Helsinki and was approved by the Ethics and Research Committee of the National Institute of Cardiology Ignacio Chavez. Reference number: PT-17-087.

Statistical analysis

Frequency distribution of categorical variables are reported as frequencies and percentages. Data is presented as mean (standard deviation) or median (interquartile range) where appropriate. To compare differences of echocardiographic parameters among pulmonary hypertension categories, we performed a one-way ANOVA or Kruskal-Wallis test whether it met assumptions of parametric tests or not, and a Dunn's post hoc test was also assessed to evaluate differences among groups.

Correlation of strain parameters with probability of pulmonary hypertension

We performed a natural logarithmic transformation in variables with non-parametric distribution. Afterward, we assessed the correlation of both RV-FWS and RA-GS with sPAP using Pearson correlation analysis to obtain the correlation coefficient using our transformed variables. To evaluate the prediction capacity of RV-FWS with sPAP, we performed polynomic adjusted linear regression analysis to assess the association between both parameters. The R2 was reported to express the variability explained by both variables. As a second step, we adjusted these models for age, sex, and body surface area as these variables could modify the relationship of RV-FWS and sPAP. As a secondary analysis, we evaluated the association of sPAP with the right heart chamber fibrosis of our second cohort sample, using the methods previously described.

Diagnostic performance of right heart chambers strain parameters

We sought to evaluate the diagnosis performance of RV-FWS and RA-GS to predict categories of pulmonary hypertension severity. Receiver operating characteristic curve (ROC) analysis curves were generated and area under the curve (AUC) derived for RV and RA strain and compared with the Fraction of Shortening, TAPSE, TEI, which are commonly used echocardiographic parameters to evaluate right heart ventricle functionality. Furthermore, we sought to identify the optimal cut-off value of the strain parameters using the "Youden method" from the R package "*Optimal cut points* " and evaluate the diagnostic test capacity, AUC, sensitivity, specificity, positive and negative predictive values (VPP, VPN, respectively) to predict pulmonary hypertension categories (14). Finally, we performed logistic regression models to assess the likelihood to have each pulmonary hypertension categories with their respective identified cut-off value. The goodness of fit of the logistic regression model was assessed using the Hosmer & Lemeshow test. All statistical analyses were performed using the R software (version 3.5.1) (15). A p -value <0.05 was considered as our statistically significant threshold.

RESULTS

Study population

We evaluated 314 patients in our study period, of which 236 had completed clinical and echocardiographic evaluation for our main analyses (**Supplementary Figure 1**). Characteristics and echocardiographic assessment of our first cohort sample are presented in**Table 1** . Briefly, our population had a male predominance (52.9%), with a mean age of 55 (+-15) years. The echocardiographic evaluation showed a median peak RV-longitudinal FWS of -26.9% (IQR: -31.2% to -21.2%) and a peak RA-GLS of 42.2% (IQR: 30.6% to 55.0%). Median systolic pulmonary arterial pressure was 33 (IQR: 28-41) mmHg. In our studied sample, 134 (56.8%) had normal sPAP values, from peak TR velocity, which represented our control group; 102 (43.2%) were classified with probability of pulmonary hypertension. Of these patients, 58 (56.9%) had low, 15 (14.7%) intermediate, and 29 (28.4%) high probability of pulmonary hypertension. Finally, in the 13 patients submitted to cardiac catheterization, we observed an acceptable inter-rater reliability coefficient (IRC: 56.8%) with echocardiographic sPAP parameters and an overall variance with the mean between both parameters [?]30% (**Supplementary Figure 2**).

Association of strain parameters with probability of pulmonary hypertension

RV-FWS absolute values were negatively correlated with SPAP (r= -0.333, 95% CI -0.215 to 0.442) as well as with RA-GLS (r= -0.432, 95% CI -0.530 to -0.322). RV-FWS and RA-GLS explained 22.2% and 18.3% of the variability of sPAP, respectively. These trends were sustained after adjusting for age, sex and BSA.

Interestingly, we observed that both parameters had a quadratic fit adjustment (**Figure 4**). Regarding the right atrial chamber assessment, the reservoir, conduit, and contractile phases had decreased parameters with advanced pulmonary hypertension categories suggesting a functional and structural decline of the RA function. However, when comparing specifically between the intermediate and high probability of PH groups, these changes where not statistically significant (**Figure 5**). This might be related to the small number of subjects classified with intermediate PH.

Association of probability of pulmonary hypertension with right chamber fibrosis

The relationship between increased sPAP values and myocardial fibrosis in right chambers was evaluated in our second cohort of postmortem samples biopsies. Clinical and echocardiographic characteristics are presented in **supplementary table 1** . sPAP had a positive correlation with right ventricular fibrosis (r= 0.671, 95% CI 0.118-0.906; p=0.024), but not with atrial fibrosis (r= 0.416, 95% CI -0.246 to 0.81; p=0.203), which explains the explained 18.3% and 8.1% of the variability of right ventricular and atrial fibrosis, respectively (**Supplementary Figure 3**).

Diagnostic Value of strain parameters in the evaluation of probability of PH

Finally, we evaluate the ability of strain parameters to predict the presence of PH and to categorize severity in patients with probability of PH. Compared with other echocardiographic parameters (RVFAC, TAPSE, TEI), both RV-FWS and RA-GS showed an adequate AUC to identify the presence of pulmonary hypertension and their respective severity categories. RA-GS outperformed other echocardiographic parameters to detect those patients with any degree of pulmonary hypertension (AUC: 0.691, 95% CI: 0.621-0.762), while RV-FWS outperformed in those with high probability of pulmonary hypertension (AUC: 0.886, 95% CI 0.832-0.940) (**Figure 6**). RV-FWS of -27.30%, -22.60%, and -22.10% had an optimal AUC and predictive test performance to predict presence of pulmonary hypertension, and to predict intermediate-to-high probability of pulmonary hypertension, and high pulmonary hypertension, respectively. Furthermore, our identified cut-off values for RA-GS were 26.30%, 34.36%, and 37.20% to detect the previously mentioned categories (**Table 2**). Using the previously identified cut-off values in our multivariate logistic regression models, we found a significantly increased likelihood for pulmonary hypertension categories, which were maintained after adjustment for covariates (**Table 3**).

DISCUSSION

In this study, we show the association of both right ventricular free wall and global right atrial strain with increased systolic pulmonary artery pressure. Moreover, we demonstrate that pulmonary arterial hypertension could be associated with myocardial fibrosis of the right heart obtained with histopathological methods. These findings suggest the association of increased sPAP values with overall ventricular deformation and fibrosis. Finally, we demonstrate that strain parameters contribute to the detection of PH and assessment of pulmonary hypertension severity in patients with suspected probability of PH.

The relationship between ventricular deformation and sPAP has been previously reported (16–18). A chronic increase in afterload, manifested by an elevated pulmonary artery pressure, can cause a decrease in the elastance of myocardial fibers in patients with severe pulmonary hypertension (17,19). This will ultimately cause irreversible myocardial damage with the eventual development of ventricular fibrosis (20). As our results suggest, the progressive decrease in ventricular strain and atrial strain is modeled as a quadratic function, which suggests that these patients have an initial period of compensation by increasing contractility, possibly via the Frank-Starling mechanism, that progressively decreases as the disease advances. This may be more pronounced in the right ventricle, as the chamber directly facing the increased afterload, before impairing the right atrium. The atrial function is also altered, as observed in the evaluation of the various atrial phases. Finally, the degree of fibrosis analyzed in the pathological specimens of a subset of patients with pulmonary hypertension was associated with a prolonged decrease in ventricular function.

With the demonstration of fibrosis, usually an irreversible change, early detection and stratification of PH is critical. Our data demonstrate the clinical utility of RV-FWS and RA-GS as echocardiographic param-

eters that aid in this task. Strain parameters have been previously used to predict outcomes in congestive heart failure and myocardial infarction with similar results (21,22), as well as in pulmonary hypertension (23,24,25). The echocardiographic estimation of sPAP and accordingly the development of the probability of PH is usually predicated on the presence of a complete tricuspid regurgitation envelope by continuous wave Doppler. Often these envelopes are incomplete and the accuracy of the sPAP estimation is markedly reduced. One usually relies on secondary signs of PH including RV dilatation, dysfunction by TAPSE or S', or D-shaped septum configuration in systole. Many of these findings are only present in advanced PH. RV strain measurement may permit for earlier detection of dysfunction, as it does in chemotherapy-induced LV cardiomyopathy (26) or in the RV in patients with scleroderma (27). In addition, strain measurements may assist in risk stratification in clinical contexts where conventional approaches are not sufficient. In our work, we identified strain cut-off values that demonstrate the differences in pulmonary hypertension severity categorization. Overall, RV-FWS offers to be a highly sensitive echocardiographic parameter while RA-GS offers a sufficient specific parameter to detect all categories of pulmonary hypertension. If our cut-off values are validated, they could be used in a clinical setting to aid detection and categorization of PH.

Strengths and limitations

Our study has some limitations. Our patients were recruited at a referral hospital, which may represent a population bias in terms of disease prevalence and severity. Despite this, our population had a significant cohort without PH and had various degrees of pulmonary hypertension. There was, however, only a small number of patients with moderate PH, potentially affecting our ability to see significantly different measurements between the moderate and severe PH categories. Additionally, we included a small cohort of patients with PH and with biopsies evaluated postmortem to determine the presence and percentage of fibrosis associated with an increase in systolic pulmonary artery pressure. We did not have strain values in these patients. Accordingly, while fibrosis has been associated with reduced echocardiographic derived strain, we consider the relationship between pathology-derived fibrosis and reduced strain as a measurement of decreased RV function and possibly of fibrosis as exploratory. Finally, the assessment at follow-up to evaluate possible adverse outcomes is left as an area of opportunity for further research.

CONCLUSION

Elevated pulmonary artery pressure is associated with dysfunction of the right atrium and right ventricle as shown by decreased RV and RA peak global longitudinal strain. We believe that this chronic dysfunction may be related to an eventual risk for fibrosis. The use of echocardiographic derived strain parameters in clinical practice could be a potential tool for detecting the presence and evaluating the probability of PH as estimated by sPAP. If validated, proposed cut-off values may improve the clinical staging of pulmonary hypertension by including a non-invasive marker of dysfunction or fibrosis.

ACKNOWLEDGMENTS: The authors would like to acknowledge all the staff of the Nuclear Cardiology Department at Instituto Nacional de Cardiologia Ignacio Chavez, particularly to the nurses and technicians. NEAV and ECG are enrolled at the PECEM program of the Faculty of Medicine, and CONACyT supports them.

CONFLICT OF INTERESTS: The authors declare that they have no conflict of interests.

AUTHORS' CONTRIBUTIONS: Research idea and study design NEZ, NEAV, EAR; data acquisition: RAS, GCC, AAF, DOC; data analysis/interpretation: NEZ, NEAV, ECG; statistical analysis: NEAV, ECG; manuscript drafting: NEZ, NEAV, LR, EAR NCN; supervision or mentorship: NEZ, LR. Each author contributed important intellectual content during manuscript drafting or revision and accepts accountability for the overall work by ensuring that questions pertaining to the accuracy or integrity of any portion of the work are appropriately investigated and resolved. NEZ, NEAV, LR, RAS, GCC, AAF, DOC, EAR

FUNDING: No funding was received.

REFERENCES

1. Zaidi A, Knight DS, Augustine DX, Harkness A, et al: Echocardiographic assessment of the right heart in adults: a practical guideline from the British Society of Echocardiography. Echo Res Pract [Internet]. 2020 Feb 27;7(1):G19–41. Available from: https://pubmed.ncbi.nlm.nih.gov/32105053

2. Habib G, Torbicki A: The role of echocardiography in the diagnosis and management of patients with pulmonary hypertension. Eur Respir Rev [Internet]. 2010 Dec 1;19(118):288 LP – 299. Available from: http://err.ersjournals.com/content/19/118/288.abstract

3. Hulshof HG, Eijsvogels TMH, Kleinnibbelink G, et al: Prognostic value of right ventricular longitudinal strain in patients with pulmonary hypertension: a systematic review and meta-analysis. Eur Heart J Cardiovasc Imaging. 2019 Apr;20(4):475–484.

4. Samarai D, Ingemansson S, Gustafsson R, Thilen U, Hlebowicz J: Global longitudinal strain correlates to systemic right ventricular function. Cardiovasc Ultrasound. 2020 Dec 1;18.

5. Rudski LG, Lai WW, Afilalo J, et al: Guidelines for the Echocardiographic Assessment of the Right Heart in Adults: A Report from the American Society of Echocardiography: Endorsed by the European Association of Echocardiography, a registered branch of the European Society of Cardiology, and the Canadian Society of Echocardiography. J Am Soc Echocardiogr [Internet]. 2010 Jul 1;23(7):685–713. Available from: https://doi.org/10.1016/j.echo.2010.05.010

6. Hamada-Harimura Y, Seo Y, Ishizu T, et al: Incremental Prognostic Value of Right Ventricular Strain in Patients With Acute Decompensated Heart Failure. Circ Cardiovasc Imaging. 2018 Oct;11(10):e007249.

7. Lee J-H, Park J-H: Strain Analysis of the Right Ventricle Using Two-dimensional Echocardiography. J Cardiovasc imaging [Internet]. 2018/08/29. 2018 Sep;26(3):111–124. Available from: https://pubmed.ncbi.nlm.nih.gov/30310878

8. Hasselberg NE, Kagiyama N, Soyama Y, et al. The Prognostic Value of Right Atrial Strain Imaging in Patients with Precapillary Pulmonary Hypertension. J Am Soc Echocardiogr. 2021;34(8):851-861.e1. doi:10.1016/j.echo.2021.03.007

9. Jones N, Burns AT, Prior DL: Echocardiographic Assessment of the Right Ventricle-State of the Art. Hear Lung Circ [Internet]. 2019 Sep 1;28(9):1339–1350. Available from: https://doi.org/10.1016/j.hlc.2019.04.016

10. Sebbag I, Rudski LG, Therrien J, Hirsch A, Langleben D: Effect of chronic infusion of epoprostenol on echocardiographic right ventricular myocardial performance index and its relation to clinical outcome in patients with primary pulmonary hypertension. Am J Cardiol 2001;88:1060-3.

11. Lang RM, Badano LP, Mor-Avi V, et al: Recommendations for cardiac chamber quantification by echocardiography in adults: an update from the American Society of Echocardiography and the European Association of Cardiovascular Imaging. J Am Soc Echocardiogr Off Publ Am Soc Echocardiogr. 2015 Jan;28(1):1-39.e14.

12. Galie N, Humbert M, Vachiery JL, et al: 2015 ESC/ERS Guidelines for the diagnosis and treatment of pulmonary hypertension. Rur Heart J 2016;37:67-119.

13. Mor-Avi V, Lang RM, Badano LP, et al: Current and evolving echocardiographic techniques for the quantitative evaluation of cardiac mechanics: ASE/EAE consensus statement on methodology and indications endorsed by the Japanese Society of Echocardiography. J Am Soc Echocardiogr Off Publ Am Soc Echocardiogr. 2011 Mar;24(3):277–313.

14. Lopez-Raton M, Rodriguez-Alvarez M, Suarez CC, Sampedro FG: "OptimalCutpoints: An R Package for Selecting Optimal Cutpoints in Diagnostic Tests." *J Statistc Softw* 2014; **61** (8), 1–36. doi: *10.18637/jss.v061.i08*.

15. Harrell F: Regression Modeling Strategies: With Applications to Linear Models, Logistic Regression, and Survival Analysis. New York, NY: Springer-Verlag; 2001.

16. Padervinskienė L, Krivickienė A, Hoppenot D, et al: Prognostic Value of Left Ventricular Function and Mechanics in Pulmonary Hypertension: A Pilot Cardiovascular Magnetic Resonance Feature Tracking Study. Medicina (Kaunas) [Internet]. 2019 Mar 20;55(3):73. Available from: https://pubmed.ncbi.nlm.nih.gov/30897834

17. Yurdakul S, Bingöl Z, Okumuş G, et al: Left Ventricular Rotational Deformation is Impaired in Pulmonary Hypertension: A Speckle Tracking Imaging- Based Study. J Am Coll Cardiol [Internet]. 2013 Oct 29;62(18 Supplement 2):C2. Available from: http://www.onlinejacc.org/content/62/18_Supplement_-2/C2.1.abstract

18. Theres L, Hübscher A, Stangl K, et al: Associations of 2D speckle tracking echocardiography-based right heart deformation parameters and invasively assessed hemodynamic measurements in patients with pulmonary hypertension. Cardiovasc Ultrasound [Internet]. 2020;18(1):13. Available from: https://doi.org/10.1186/s12947-020-00197-z

19. Lan NSH, Massam BD, Kulkarni SS, Lang CC: Pulmonary Arterial Hypertension: Pathophysiology and Treatment. Dis (Basel, Switzerland) [Internet]. 2018 May 16;6(2):38. Available from: https://pubmed.ncbi.nlm.nih.gov/29772649

20. Collum SD, Amione-Guerra J, Cruz-Solbes AS, et al: Pulmonary Hypertension Associated with Idiopathic Pulmonary Fibrosis: Current and Future Perspectives. Can Respir J [Internet]. 2017/02/13. 2017;2017:1430350. Available from: https://pubmed.ncbi.nlm.nih.gov/28286407

21. Salvo G Di, Pergola V, Fadel B, Bulbul Z Al, Caso P: Strain Echocardiography and Myocardial Mechanics: From Basics to Clinical Applications. J Cardiovasc Echogr [Internet]. 2015;25(1):1–8. Available from: https://pubmed.ncbi.nlm.nih.gov/28465921

22. Kaufmann D, Szwoch M, Kwiatkowska J, Raczak G, Daniłowicz-Szymanowicz L: Global longitudinal strain can predict heart failure exacerbation in stable outpatients with ischemic left ventricular systolic dysfunction. PLoS One [Internet]. 2019 Dec 2;14(12):e0225829–e0225829. Available from: https://pubmed.ncbi.nlm.nih.gov/31790492

23. Nathaniel R: Right Ventricular Strain in Pulmonary Hypertension. Circ Cardiovasc Imaging [Internet]. 2013 Sep 1;6(5):609–611. Available from: https://doi.org/10.1161/CIRCIMAGING.113.000936

24. Fine NM, Chen L, Bastiansen PM, et al: Outcome Prediction by Quantitative Right Ventricular Function Assessment in 575 Subjects Evaluated for Pulmonary Hypertension. Circ Cardiovasc Imaging [Internet]. 2013 Sep 1;6(5):711–721. Available from: https://doi.org/10.1161/CIRCIMAGING.113.000640

25. Shukla M, Park J-H, Thomas JD, et al: Prognostic Value of Right Ventricular Strain Using Speckle-Tracking Echocardiography in Pulmonary Hypertension: Systematic Review and Meta-analysis. Can J Cardiol [Internet]. 2018 Aug 1;34(8):1069–1078. Available from: https://doi.org/10.1016/j.cjca.2018.04.016

26. Thavendiranathan P, Poulin F, Lim KD, Plana JC, Woo A, & Marwick TH: Use of myocardial strain imaging by echocardiography for the early detection of cardiotoxicity in patients during and after cancer chemotherapy: a systematic review. J Am Coll Cardiol. (2014) 63(25 Pt A), 2751–2768. https://doi.org/10.1016/j.jacc.2014.01.073

27. Mukherjee M, Mercurio V, Tedford RJ, Shah A A, et al: Right ventricular longitudinal strain is diminished in systemic sclerosis compared with idiopathic pulmonary arterial hypertension. *Eur Resp J.* 2017; *50* (5), 1701436. https://doi.org/10.1183/13993003.01436-2017

FIGURES

Figure 1. Apical four-chamber view showing the right atrial global longitudinal strain (RA-GS) with the measurement of reservoir (A), conduit (B) and contractile (C) strain phases.

Figure 2 . A) Specimen showing the internal appearance of the dilated right atrium, the pectinate portion that continues with the appendage is observed to the right of the observer and the anterior leaflet of the tricuspid valve is observed below. B) Transthoracic 3D echocardiogram in four chamber view with mild enlargement of right atrium. C) Mild pulmonary hypertension SPAP of 44 mmHg. D) Histological study (stained with Masson, 10X) of the atrial myocardium of a patient, with mild pulmonary hypertension. The muscle fascicles were mostly cut transversely or obliquely. Two muscle fascicles are replaced by fibrous connective tissue rich in collagen fibers that stain blue, and contrast with the red in which the myocardium is stained. One fascicle is partially replaced by collagen and another almost entirely. The degree of fibrosis in the observed fields was calculated at 25%, since in this image it could reach a little more than a quarter. E) Echocardiography with velocity vector imaging of a patient with low probability of pulmonary hypertension, who had a normal global longitudinal strain of the right atrium (43.5%). *Abbreviations* : RA-right atrium, RV-right ventricle.

Figure 3. A) Specimen of the heart of a patient with sPAP of 90 mmHg. Heart cut longitudinally from the atria to the ventricles (entry routes through the postero-inferior aspect) that allows to appreciate the dilation of the right cavities. B) Two-dimensional echocardiogram with Doppler in the apical 4-chamber view, with severe tricuspid regurgitation, by means of which an average gradient of 77 mmHg was calculated. C) In the subcostal plane, dilatation of the inferior vena cava (29.1 mm) and collapse of $<$50% were detected, calculating a right atrial pressure was of 15 mmHg. D) Histological study of the right ventricular myocardium, most of the muscle fibers are in longitudinal section in red and the fibrous tissue rich in collagen fibers is observed blue, it extensively replaces the muscle fascicles, and, in this image, it reaches 75 % or three quarters. The muscle fibers embedded in the fibrous connective tissue appear elongated and thinned. Masson 10x.

E) The global longitudinal strain of the right ventricle, using velocity vector imaging was -14%, in a patient with high probability of PH (sPAP=92 mmHg). Abbreviations: RA-right atrium, RV-right ventricle, LA-left atrium, LV-left ventricle.

Figure 4. Correlation of the absolute values of RV-FWS (A) and RA-GS (B) with logarithmical sPAP. *Abbreviations* : sPAP: systolic pulmonary artery pressure; RV-FWS: Right ventricular free wall Strain; RA-GS: Right atrial global longitudinal strain.

Figure 5. Differences amongst right atrial reservoir (A), conduit (B) and contractile (C) phases in pulmonary hypertension categories. *Abbreviations* : sPAP: systolic pulmonary artery pressure; RV-FWS: Right ventricular free wall strain; RA-GS: Right atrial global longitudinal strain.

Figure 6. ROC with the area under the curve of echocardiographic parameters to identify the discrimination capacity for low (A) intermediate/high (B) and high (C) probability of pulmonary hypertension. *Abbreviations* : ROC= Receiver operator characteristic; Frac-Short= Fractional shortening; TAPSE= Tricuspid annular plane systolic excursion; TEI= TEI index; RV-FWS: Right ventricular free wall strain; RA-GS: Right atrial global longitudinal strain.

Supplementary Figure 1. Algorithm for patients' selection

Supplementary Figure 2. Correlation of RV-Fibrosis (A) and RA-Fibrosis (B) with sPAP. *Abbreviations* : sPAP: Systolic pulmonary artery pressure; RV-FWS: Right ventricular free wall strain; RA-GS: Right atrial global longitudinal strain.

Supplementary Figure 3. Correlation of sPAP using echocardiographic and right hearth catheterization (A) and Bland-Altman plot with observed differences between both methods of measured sPAP (B). *Abbreviations* : sPAP: systolic pulmonary artery pressure.

Table 1: Echocardiography assessment of population of study.*Abbreviations* : BSA: Body surface area; RVd: Right Ventricle Diameter; FAC: Fractional area change; TAPSE: Tricuspid annular plane systolic excursion; RVS: right ventricular Synchrony.

Parameter	**n=236**
Male (%)	124 (52.9%)
Age (years)	54.6 (±15.6)
Height (cm)	1.62 (±0.1)
Weight (kg)	71.8 (±15.4)
BSA (cm)	1.75 (1.62-1.90)
Right Ventricle	
RVd (mm)	36 (33-40.2)
RVFAC (%)	40.4 (35-48)
TAPSE (mm)	20 (17.4-22)
RV-Synchrony (ms), n=141	22 (3.5-44)
TEI index	0.53. (±0.17)
E Wave (cm/s), n=141	9.0 (7-12)
A Wave (cm/s), n=141	13 (9.25-16)
S Wave (cm/s), n=141	11 (9.8-12.4)
E/A, n=141	0.76 (0.62-0.94)
Right Atrium	
Volume (ml/m^2)	31 (21-44)
Area (cm2)	14 (11.6-17)
Reservoir Phase (%)	41.7 (30.3-55)
Conduit Phase (%)	22 (13.4-30)
Contractile Phase (%)	18.8 (13.3-26.9)
sPAP (mmHg) n=233	33 (28-41)
PH Categories	
No-PH (%)	131 (55.5)
With-PH Mild (%) Moderate (%) Severe (%)	102 (43.2) 58 (56.9) 15 (14.7) 29 (28.4)
Ventricular and atrial strain	
RV-FWS (%)	-26.86 (-21.2 to -31.22)
RA-GS (%)	42.2 (30.6 - 55)

Table 2: Cut-off values and predictive tests using RV-FWS for pulmonary, intermediate /high, and high probability of pulmonary hypertension. *Abbreviations* : RV-FWS= Right-ventricular Free-Wall Strain; AUC= Area under the curve; SE= Sensitivity; SPE= Specificity; PLR= Positive likelihood ratio; NLR= Negative likelihood ratio; PPV= Positive predictive value; NPV= Negative predictive value.

Outcome	Parameter	Cut-Off	SE	SPE	PPV	NPV	LR+	LR-	AU
Pulmonary Hypertension	RV-FWS	-27.30	0.700 (0.600-0.787)	0.569 (0.479-0.655)	0.555 (0.465-0.665)	0.711 (0.613-0.780)	1.62 (1.28-2.05)	0.527 (0.37-0.73)	0.6 (0. 0.7
Intermediate-High PH		-22.60	0.773 (0.621-0.88)	0.801 (0.736-0.855)	0.479 (0.389-0.676)	0.937 (0.878-0.956)	3.88 (2.79-5.40)	0.284 (0.16-0.49)	0.8 (0.
High PH		-22.10	0.896 (0.726-0.978)	0.791 (0.728-0.845)	0.382 (0.304-0.761)	0.981 (0.942-0.987)	4.29 (3.19-5.76)	0.131 (0.044-0.38)	0.8 (0. 0.9
Pulmonary Hypertension	RA-FWS	26.30	0.809 (0.731-0.873)	0.515 (0.413-0.615)	0.683 (0.589-0.777)	0.675 (0.572-0.758)	1.67 (1.342-2.072)	0.371 (0.248-0.553)	0.6 (0. 0.7

Outcome	Parameter	Cut-Off	SE	SPE	PPV	NPV	LR+	LR-	AU
Intermediate-High PH		34.36	0.793 (0.728-0.848)	0.773 (0.621-0.885)	0.937 (0.878-0.956)	0.466 (0.378-0.664)	3.487 (2.012-6.042)	0.268 (0.194-0.370)	0.8 (0. 0.9
High PH		37.20	0.679 (0.611-0.743)	0.862 (0.683-0.961)	0.972 (0.922-0.979)	0.277 (0.221-0.603)	4.928 (1.97-12.30)	0.371 (0.289-0.476)	0.8 (0. 0.8

Table 3: Logistic regression model to predict intermediate/high PH using identified cut-off values for each outcome adjusted for sex, age and BSA. Abbreviations: BSA= body surface area; RV= Right Ventricle; RA= Right Atrium.

Model	**Parameter**	**B**	**SE**	**Wald**	**OR (95% CI)**	**P value**
Pulmonary Hypertension	RV-FWS >-27.30	1.402	0.311	4.497	4.06 (2.23-7.63)	<0.001
	RA-GS < 26.30	2.701	0.474	5.699	14.90 (6.22-40.66)	<0.001
Intermediate-High probability of Pulmonary Hypertension	RV-FWS >-22.60	2.687	0.441	6.088	14.69 (6.43-36.74)	<0.001
	RA-GS <34.36	2.830	0.457	6.18	16.95 (7.23-44.12)	<0.001
High probability of Pulmonary Hypertension	RV-FWS >-22.10	3.682	0.683	5.391	39.73 (11.96-187.05)	<0.001
	RA-GS <37.20	2.778	0.599	4.635	16.10 (5.50-60.48)	<0.001

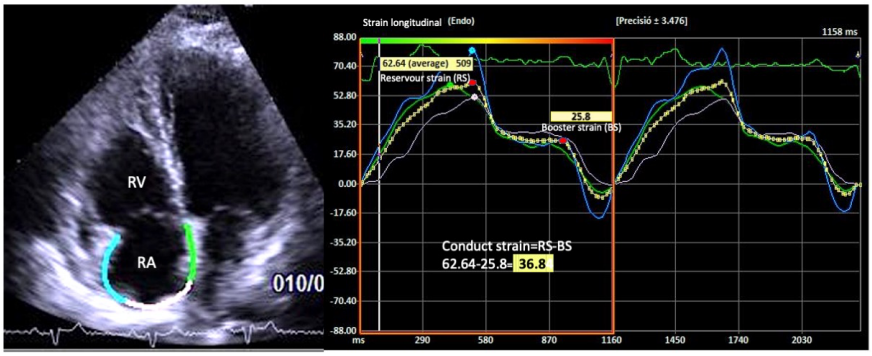

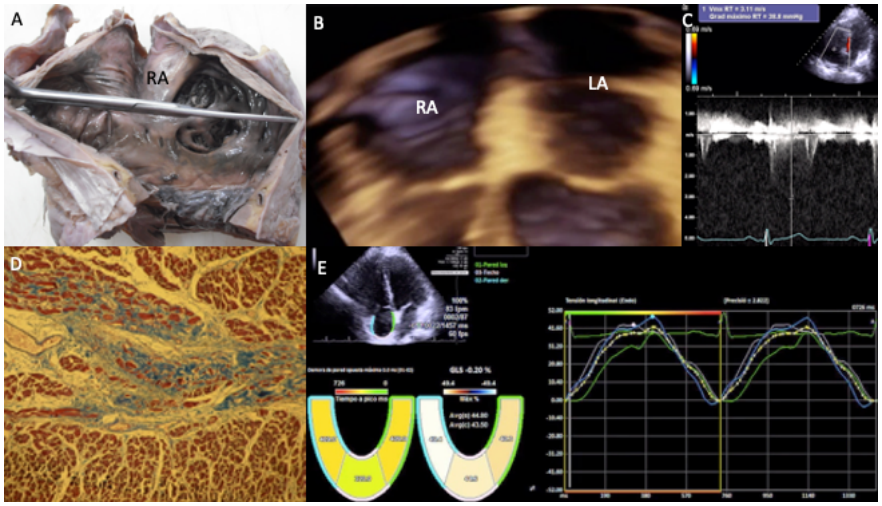

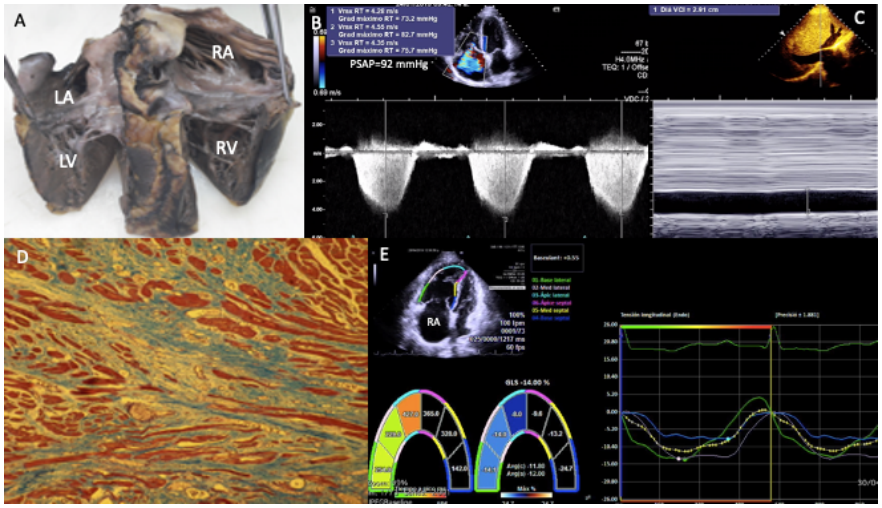

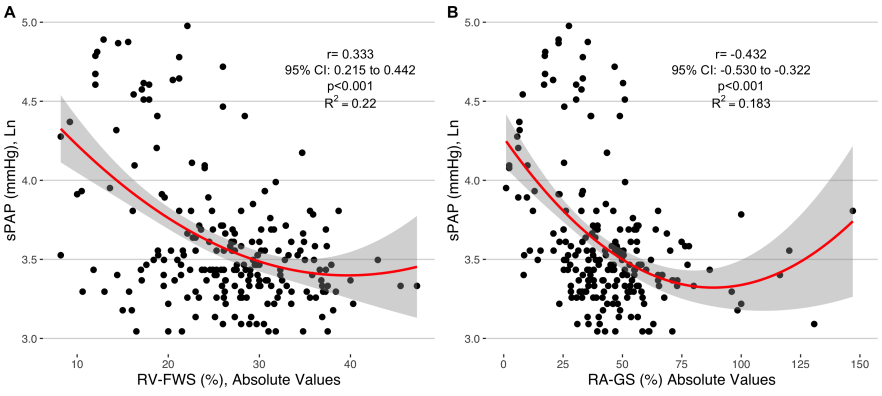

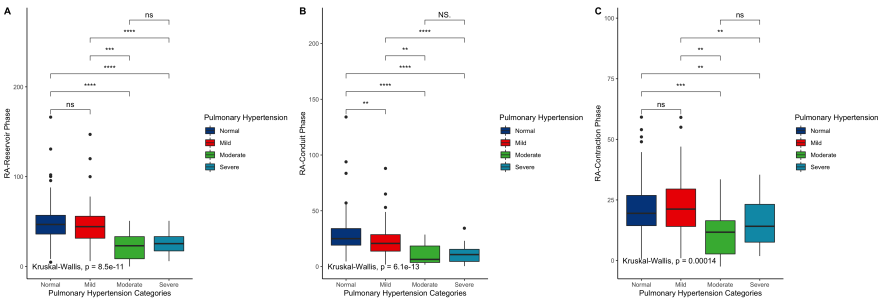

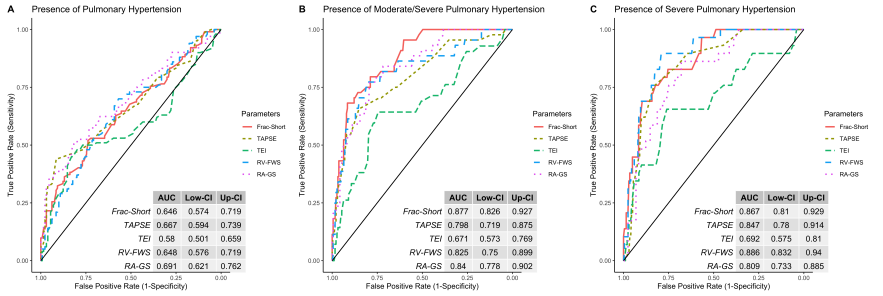

	AUC	Low-CI	Up-CI
Frac-Short	0.646	0.574	0.719
TAPSE	0.667	0.594	0.739
TEI	0.58	0.501	0.659
RV-FWS	0.648	0.576	0.719
RA-GS	0.691	0.621	0.762

	AUC	Low-CI	Up-CI
Frac-Short	0.877	0.826	0.927
TAPSE	0.798	0.719	0.875
TEI	0.671	0.573	0.769
RV-FWS	0.825	0.75	0.899
RA-GS	0.84	0.778	0.902

	AUC	Low-CI	Up-CI
Frac-Short	0.867	0.81	0.929
TAPSE	0.847	0.78	0.914
TEI	0.692	0.575	0.81
RV-FWS	0.886	0.832	0.94
RA-GS	0.809	0.733	0.885